можливість застосування побудованої теорії для розрахунків спектрів феромагнітних нанодротів.

ВИСНОВКИ

В роботі була представлена оригінальна модифікована еліптична система координат, розглянуто її основні властивості, знайдено масштабні множники Ламе, побудовано координатні поверхні, записано вирази для диференціальних операторів градієнта, ротора, дивергенції та оператора Лапласа. Запропоновано використовувати модифіковану еліптичну систему координат при розв'язанні задач математичної фізики в системах з геометрією еліптичного циліндра і наведено приклади успішного застосування.

ПЕРЕЛІК ПОСИЛАНЬ

1. *Mahmoud S. F.* Electromagnetic waveguides: theory and applications / S. F. Mahmoud. – London : Peter Peregrinus Ltd., 1991. – 228 p.
2. *Dyott R. B.* Elliptical Fiber Waveguides / R. B. Dyott. – Norwood, MA : Artech House, 1995. – 217 p.
3. *De Wames R. E.* Magnetostatic surface modes in an axially magnetized elliptical cylinder / R. E. De Wames, T. Wolfram // Appl. Phys. Lett. – 1970. – Vol. 16, № 8. – P. 305–308.
4. *Анго А.* Математика для электро- и радиоинженеров / А. Анго. – М. : Наука, 1965. – 779 с.
5. Иванов В. И. Конформные отображения и их приложения / В. И. Иванов, В. Ю. Попов. – М. : Едиториал УРСС, 2002. – 324 с.
6. *Miyazaki Y.* Radio Wave absorption analysis of coated elliptic cylinders with lossy magnetic ferrite films using conformal mapping method / Y. Miyazaki // 3rd International Symposium on Electromagnetic Compatibility. – Beijing (China), 2002. – P. 432–437.
7. *Roussigne Y.* Spin waves in stripe submitted to a perpendicular applied field / Y. Roussigne, P. Moch // J. Phys. Condense Matter. – 2005. – Vol. 17, № 10. – P. 1645–1652.
8. *Гуревич А. Г.* Магнитные колебания и волны / А. Г. Гуревич, Г. А. Мелков. – М. : Физматлит., 1994. – 464 с.
9. *Зависляк И. В.* Поверхностные магнитостатические колебания в эллиптических отверстиях и цилиндрах / И. В. Зависляк, Г. П. Головач, М. А. Попов, В. Ф. Романюк // РЭ. – 2006. – Т. 51, № 2. – С. 213–220.
10. *Попов М. А.* Поверхностные магнитостатические колебания в ферритовых трубках эллиптического сечения / М. А. Попов, И. В. Зависляк // Известия вузов. Радиоэлектроника. – 2006. – Т. 49, № 6. – С. 3–11.
11. *Попов М. А.* Modelling of the magnetostatic surface oscillations in elliptical nanotubes / М. А. Попов, И. В. Зависляк // УФЖ. – 2008. – Т. 53, № 7. – С. 706–711.
12. *Попов М. А.* Поверхностные магнитостатические колебания в эллиптических цилиндрических магнитных доменах / М. А. Попов, И. В. Зависляк // ФТТ. – 2009. – Т. 51, № 1. – С. 81–84.

Надійшла 7.04.2009
Після доробки 28.05.2009

Представлена оригинальная модифицированная эллиптическая система координат, рассмотрены ее свойства, приведены полезные соотношения. Предложено использовать эту систему координат при рассмотрении задач математической физики с симметрией эллиптического цилиндра, в частности, задач про нахождение собственных волн и колебаний в волноводах и резонаторах эллиптического сечения, продемонстрированы примеры ее применения.

The original modified elliptical coordinate system is submitted, its properties are considered, useful relationships are given. It was suggested to use this coordinate system for mathematical physics problems with the symmetry of the elliptical cylinder, in particular for eigenwaves and eigen oscillations problems in waveguides and of elliptic cross-section resonators, the examples of application were demonstrated.

УДК: 538.935, 538.915, 538.953

V. V. Pogosov, E. V. Vasyutin, A. V. Babich

FEATURE OF MAGIC METAL NANOCLUSTERS IN MOLECULAR TRANSISTOR

Effects of the charging and single-electron tunneling in a cluster structure are investigated theoretically. In the framework of the particle-in-a-box model for the spherical and disk-shaped gold clusters, the electron spectrum and the temperature dependence of the electron chemical potential are calculated. Difference between the chemical potentials of massive electrodes and island's one leads to its charging. We show that the effective residual charge is equal to the non-integer value of elementary charge e and depends on the cluster's shape. The equations for the analysis of the current-voltage characteristic are used under restrictions associated with the Coulomb instability of a cluster. For single-electron molecular transistors the non-monotonic size dependences of current gap and its voltage asymmetry are computed. We suggest that an overheating of electron subsystem leads to the disappearance of a current gap and gradual smoothing of current-voltage curves that is observed experimentally.

1 INTRODUCTION

The nanodispersed systems are prospective object of nanotechnology [1, 2, 3, 4, 5, 6]. Transport of electrical charge across a nanoscale tunnel junction is accompanied by many effects, such as the Coulomb blockade of the average current, transfer of energy between elec-

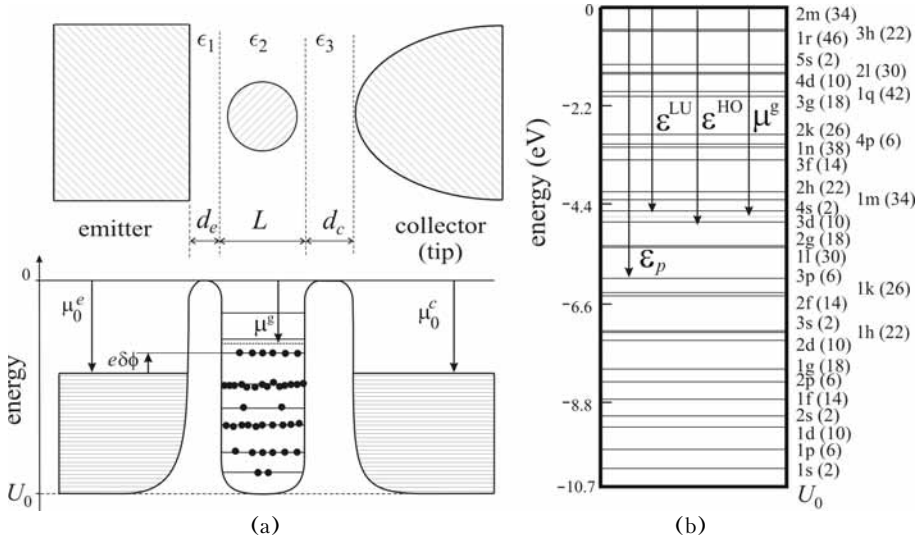

Figure 1:
(a) The energy diagram at $T = 0$ for the structure $Au/Au_{40}/Au$ before application of voltage. In experiments [11, 12, 13, 14, 15] $\epsilon_1 = \epsilon$, $\epsilon_2 = \epsilon_3 = 1$;
(b) The energy spectrum for spherical magic cluster Au_{196}

trons and ions, and consequent heating of the junction [7, 8, 9]. In nanometer scale devices, electron transport can occur through well-resolved quantum states (e. g. single-electron transistor based on CdSe quantum rods [10]). If the temperature is increased, the Coulomb and quantum staircases of current are gradually smeared out by thermal fluctuations.

The tunneling current flowing through two massive electrodes can be controlled, if a cluster is placed between them. At first sight, the probability of electron tunneling (and consequently a value of the current) should be much greater in the presence of a granule between the reservoirs, than in the case of its absence. However, an opposite behavior (see inset in Fig. 2(a) of Ref. [11]) was observer in experiments for the spherical-like [11, 12, 13] and disk-shaped [14, 15] small clusters. Measured $I-V$ characteristics have a plateau of the zero current (a current gap). The metal-dielectric transition for gold cluster can appears [16].

Simple tunnel construction can be schematically represented by the distinctive "sandwich" [11, 12, 13, 14] (see Fig. 1). It consists of a thick gold film (emitter) covered by a dielectric one (with dielectric constant $\epsilon \approx 3$). Disc-shaped [14] or spherical-like [13] gold clusters are self-organized on the dielectric layer (on the detecting and manipulating single molecules with STM see in Ref. [17]). Also, a tip of STM is used in the capacity of the third electrode (collector).

The experiments demonstrated the following features of the $I(V)$ behavior:

1. The gap width of the zero conductance is *approximately* proportional to the *inverse radius* of the spheres (Figs. 1(c) and 2(a) in Ref. [11]) and disks (Fig. 4 in Ref. [14]). This does not allow one to establish unequivocally classical or quantum origin of the gap. On the other hand, out of the current gap, the steps of the staircase are clearly visible (Fig. 3 in Ref. [14] and Fig. 1(b) in Ref. [15]).

2. For a disk, the gap width varies non-monotonically with alteration of the collector-cluster distance under the fixed emitter-cluster one (Fig. 3 in Ref. [15]).

3. The observed current gap decreases significantly as temperature increases from 5 K to 300 K in structure based on disk-shaped cluster of $2R \approx 40$ A (Fig. 2 in Ref. [14]).

Some of the experimental features of the $I-V$ curves were investigated in Ref. [18], however, the fact of smoothing of staircases for granule-molecule at low temperatures is still not understood. Such a smoothing is typical for molecular transistors [19].

Using the measured $I(V)$ dependence, the capacitances and resistances of the tunnel junctions and the "residual" (fractional) charge Q_0 of a grain were fitted in Ref. [12] according to the circuit approach proposed in "orthodox" theory [1]. We propose another way: to use the self-capacitance and to fit the temperature of granule.

The aim of this work is the computation of the current-voltage characteristic of the molecular transistor based on metal clusters. For this purpose, we use some results of physics for charged metal clusters [20]. The temperature features of the $I-V$ curves are explained by overheating of electron subsystem.

The structure of a granule (or cluster) changes as more and more atoms condense together. A fundamental

characteristic of metal clusters, that researchers must explain, is why certain sizes occur preferentially. The elements of the periodic table have heightened stability because those atoms possess a special number of electrons (magic numbers). The tendency for clusters to form in exactly magic sizes arises from the rules of quantum mechanics, which dictate that bound electrons can have only certain energies. So the existence of magic numbers for metal clusters makes sense: they correspond to the number of valence electrons which completely fill one or more shells in a cluster and make it especially stable, by analogy with filled proton and neutron energy shells in atomic nuclei [21]. The calculated magic numbers depend from the shape of cluster (i. e. on the configuration of the ions).

2 FORMULATION OF THE PROBLEM

We consider spherical gold clusters whose radii vary in the range $2R \cong \{14, 28\}$ Å, $R = N_0^{1/3} r_0 \Rightarrow N_0 \cong \cong \{100, 600\}$, where N_0 is the number of atoms, r_0 is the atom density parameter, ($r_0 = 3.01 a_0$ for gold, a_0 is the Bohr radius). Similarly for disks of monatomic thickness: $2R \cong \{10, 98\}$ Å $\Rightarrow N_0 \cong \{14, 10^3\}$.

The characteristic Coulomb energy of charging is $\tilde{E}_C = e^2/C$ where C is self-capacitance of single granule in a vacuum (in the case of a disc, the capacitance can be estimated as for the oblate spheroids of equal volume [20]). The calculations of Ref. [18] demonstrated that these C are too small for the width of the current gap to be explained. The most obvious example is the case of a disc, since almost half of the disc surface contacts to the dielectric film. Therefore, for these granules we change $C \Rightarrow (1 + \epsilon)C/2$. Then, for discs and spheres we have $E_C \cong \{1.60, 0.21\}$ and $\{1.82, 1.06\}$ eV, respectively. We note that the value of the capacitance is sensitive to the shape of the granule surface, and even small deviation from the spherical shape can change significantly the capacitance. Temperature of structures (thermostat) is $T \cong 30$ K. This enhances the importance of quantum mechanical effects.

Let's determine the electron spectrum in spherical and cylindrical wells (see Appendix A). The calculation of the electron spectrum in the cylindrical and spherical wells of the mentioned sizes with finite deepness yields different values for the spectrum discreteness in magic clusters $\Delta\varepsilon_p = \varepsilon^{\mathrm{LU}} - \varepsilon^{\mathrm{HO}}$ (see Fig. 2). In the nonmagic clusters the levels of lowest unoccupied states coincide with those of highest occupied ones, $\varepsilon^{\mathrm{LU}} = \varepsilon^{\mathrm{HO}}$ at $T = 0$.

Thus, for the whole range of R in experiments [11, 12, 13, 14] we have to deal with a set of open 0D systems (quantum dots). The resulting inequality,

$$E_C \approx \Delta\varepsilon_p \gg k_B T, \qquad (1)$$

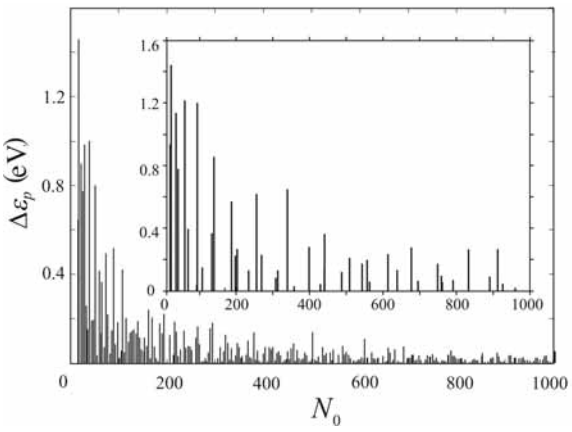

Figure 2 – Calculated specific difference between energies of lowest unoccupied electron state ε^{LU} and highest occupied one ε^{HO} in neutral discs and spheres (inset) Au_{N_0} *at* $T = 0$

corresponds, apparently, to two coexisting structures at $I-V$ curves: effects of the spectrum quantization and the Coulomb blockade. However, detailed measurements in Refs. [2, 11, 12, 13, 22] performed to date do not yield an unequivocal conclusion about the effect of electron quantization levels upon the $I(V)$. In our opinion, the discreteness of the spectrum actually determines the zero conductance gap of the $I-V$ curves observed in Refs. [11, 12, 13, 14, 15].

3 SEMICONDUCTOR-LIKE BEHAVIOR OF MAGIC METAL CLUSTER

The left and right electrodes (emitter and collector) represent the electron reservoirs. Each reservoir is taken to be in thermal equilibrium. A continuum of states is assumed in reservoirs, occupied according to the Fermi-Dirac distribution

$$f(\varepsilon^{e,c} - \mu_0^{e,c}) = \{1 + \exp[(\varepsilon^{e,c} - \mu_0^{e,c})/k_B T]\}^{-1}, \quad (2)$$

where $\mu_0 < 0$ is the electron chemical potential for a semi-infinite metal, $-\mu_0 = W_0$, W_0 is the electron work function ($W_0 = 5.13$ eV for Au). In all cases energy $U_0 < \varepsilon < 0$ is counted off from the vacuum level, $U_0 < 0$ is the position of conductivity band of a semi-infinite metal [20].

The electron chemical potential μ^g of a granule in a quantum case can be defined by the normalization condition

$$\sum_{p=1}^{\infty} f(\varepsilon_p - \mu^g) \equiv \sum_{p=1}^{\infty} \{1 + \exp[(\varepsilon_p - \mu^g)/k_B T]\}^{-1} = N_0, \quad (3)$$

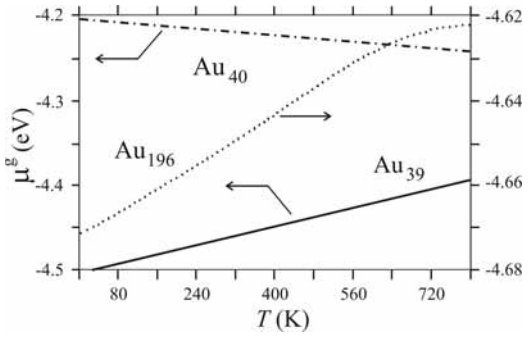

Figure 3 – Temperature dependence of chemical potentials of the neutral spherical gold non-magic (Au_{39}) *and magic* (Au_{40}, Au_{196}) *clusters*

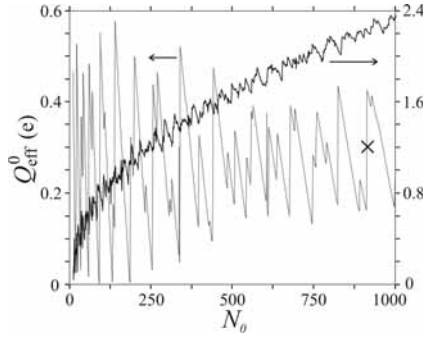

Figure 4 – The calculated size dependence of the residual effective charge Q^0_{eff} *(5) for the structure* $Au/Au_{N_0}/Au$ *based on the clusters of various shape: sphere (dotted line) and disk (solid line). For illustration,* Q^0_{eff} *of magic sphere* Au_{912} *is marked as* ×

where sum runs over all one-electron states, N_0 is the total number of thermalized electrons in a cluster, $\mu^g \equiv \mu^g(R)$. If the electron spectrum is known, from Eq. (3) it is possible to calculate μ^g of cluster Au_{N_0} (gold is univalent).

Fig. 3 depicts the chemical potential of some spherical clusters as a function of temperature. Predictably, the dependence is slack and is completely determined by the level hierarchy in dots, and also by the number of electrons.

For the magic clusters as for an intrinsic semiconductor, which has equal numbers of electrons in the conduction band and holes in the valence band, the chemical potential lie halfway between the lowest unoccupied level ε^{LU} and highest occupied one ε^{HO}, regardless of the temperature, because each electron promoted to the lowest unoccupied level leaves a hole in the highest occupied term. The Fermi level of non-magic clusters coincides with a real level in a cluster. Calculations show, that the temperature gradient of chemical potential can be both the positive and the negative, and at some temperatures it can change a sign. Similar behavior $\mu^g(N_0, T)$ for magic clusters Na_{N_0} have been reported in Ref. [23].

A contact potential difference appears between a cluster and electrodes is

$$\delta\phi = (\mu^g - \mu_0^e)/e. \qquad (4)$$

An equilibrium is reached by the charging of a cluster since it capacitance is finite. If $|\mu^g| < |\mu_0^e|$, a cluster is charged positively by a charge $Q^0_{\text{eff}} = -e(N' - N_0) > 0$, where N' is determined by the solution of the Eq. (3) with replacement $\mu^g \to -W_0$ for the same spectrum $\{\varepsilon_p\}$ shifted on $-e\delta\phi$, according to the Koopmans' theorem [20]. Thus, in thermodynamic limit we have

$$Q^0_{\text{eff}} = C\delta\phi. \qquad (5)$$

The existence of Q^0_{eff} has to do with the transparency of the tunnel barriers before application of voltage. A quasi-classical approximation [24, 25] gives for a metallic sphere of radius R: $\mu^g - \mu_0 = \mu_1/R$, $\mu_1 = 1.9$ eV$\times a_0$, $Q^0_{\text{eff}} = +0.07e$. In a quantum case, filling levels by electrons we find a highest occupied state, $\varepsilon^{\text{HO}} < 0$, and lowest unoccupied state, $\varepsilon^{\text{LU}} < 0$, counted off from the vacuum level (Fig. 1). Then it is necessary to make a replacement $\mu^g \to \varepsilon^{\text{HO}}$.

In accordance with our previous results [24], $|\mu^g| < |\mu_0|$, therefore the cluster is charged positively before the application of voltage. The size dependence of a charge $Q^0_{\text{eff}}(N_0)$ for referred gold clusters is demonstrated on Fig. 4. For the above mentioned sizes of spherical clusters, $Q^0_{\text{eff}} < e$. However, Q^0_{eff} can accept a values larger then e for the disks of monatomic thickness. Additional charging of the cluster can lead to the Coulomb instability, because the quantity Q^0_{eff} is close to a critical charge [20]. Moreover, cluster's anomalous electrostriction is possible as a result of the charging [26].

Otherwise, in the case $|\mu^g| > |\mu_0|$ (e. g. $Pb/Au_{N_0}/Pb$) the cluster is charged negatively and it is necessary to make a replacement $\mu^g \to \varepsilon^{\text{LU}}$. Residual effective charge is equal to non-integer elementary charge e, which is analogous to the charge of cluster in "chemisorption regime".

The possibility of a fractional charge at tunneling structures was discussed in Ref. [27]. Perhaps, this problem is related to the fractional quantization (or fractional statistics), when the decoupling of the spin and the electron quantum numbers of a charge is important. In the percolation systems it is supposed that the charge at the each granule has a soliton origin. The value of this charge was calculated numerically in Ref. [28].

We consider a central electrode-granule in an external electric field. Between the emitter ($V = 0$) and the

collector the positive voltage V is applied. In a weak electric field approach we assume, that the ionic subsystem of a granule is not deformed, and the electronic "cloud", generated by the own valence electrons, is deformed only.

4 GRANULE UNDER VOLTAGE V

The total energy of a granule is the functional of nonhomogeneous electron concentration, $\tilde{E}[n(\mathbf{r})]$. The functional contains a contribution responsible for the interaction of electrons and ions with an external field,

$$e\int[n(\mathbf{r})-n_i(r)](\mathbf{E}\cdot\mathbf{r})d^3r. \qquad (6)$$

For simplicity, we suppose that the charge distribution $n_i(r)$ of the ion subsystem is spherically symmetric.

Let's write down an electron distribution of a granule as

$$n(\mathbf{r}) = n_0(r) + \delta n_1(r) + \delta n_2(\mathbf{r}). \qquad (7)$$

Here, $n_0(r)$ is the electron density of neutral cluster in the absence of the external field,

$$\int n_0(r)d^3r = N_0,$$

δn_1 is the perturbation arising from the charging of granule,

$$\int \delta n_1(r)d^3r = \Delta N, \qquad (8)$$

where $\Delta N > 0$ and $\Delta N < 0$ correspond to negatively and positively charged granule, respectively ($|\Delta N| = N_0$). $\delta n_2(\mathbf{r})$ is the next perturbation arising from the external field which responses for the polarization of a neutral granule,

$$\int \delta n_2(\mathbf{r})d^3r = 0. \qquad (9)$$

We assume, that functions $n_0(r)$ and $n_1(r)$ are spherically symmetrical, and $n_2(\mathbf{r})$ is axially symmetrical. Then one can expand the $\tilde{E}[n(\mathbf{r})]$ in the functional Taylor series down to the second order of smallness with respect to δn_1 and δn_2,

$$\tilde{E}[n(\mathbf{r})] = \tilde{E}[n_0(\mathbf{r})] + \sum_j \int \frac{\delta E}{\delta n(\mathbf{r})}\delta n_j(\mathbf{r})d^3r + \\ + \frac{1}{4}\sum_{j,k}\iint \frac{\delta^2\tilde{E}}{\delta n_j(\mathbf{r})\delta n_k(\mathbf{r}')}\delta_j n(\mathbf{r})\delta n_k(\mathbf{r}')d^3rd^3r' + \ldots \qquad (10)$$

Here the functional derivatives are taken at $n(\mathbf{r}) = n_0(r)$, and indexes j and k runs 1 and 2 according to the definition (7). The zeroth-order expression $\tilde{E}[n_0(\mathbf{r})] \equiv \tilde{E}_{00}$ is a total energy of a cluster before the charging ($\Delta N = 0$) and in the absence of the external field ($E = 0$). The functional derivative

$$\delta\tilde{E}/\delta n(\mathbf{r}) = \mu^g + e(\mathbf{E}\cdot\mathbf{r}). \qquad (11)$$

In the absence of charging and external field $-\mu^g \to W_0$ as $R \to \infty$.

Finally, in the semiclassical approximation (see Appendix B), we get

$$\tilde{E} = \tilde{E}_{00} + \mu^g\Delta N - e\Delta N\eta V + (\Delta N)^2\tilde{E}_C/2 - \alpha E^2/2. \qquad (12)$$

Solving separately the electrostatic problem for the same structure with fraction of the voltage $\eta V > 0$ (Fig. 1), we obtain

$$\eta = \frac{\epsilon_2\epsilon_3(d_e + \epsilon_1 L/2\epsilon_2)}{\epsilon_1\epsilon_2 d_c + \epsilon_1\epsilon_3 L + \epsilon_2\epsilon_3 d_e} \equiv \eta^+. \qquad (13)$$

Here, $L \equiv 2R, H$ for a sphere of radius R and a disk of thickness H, respectively. We describe the situation for $\epsilon_1 \equiv \epsilon$, $\epsilon_2 = \epsilon_3 = 1$. Under Eq. (13) one can find the values $\eta^+ < 0.65$ and $\eta^+ < 0.55$ in experiments [11, 12, 13, 14, 15] for the spherical-like and disk-shaped clusters, respectively.

Now we examine the problem of critical surplus charges of a cluster in the presence of an external voltage. For convenience, further we write $n \equiv \Delta N$.

5 COULOMB INSTABILITY OF A CLUSTER IN ELECTRIC FIELD

It is necessary to note, that even the vanishing external electric field leads to the instability of a cluster because of the possibility of electron tunneling. We assume, that a cluster relaxed in a metastable state over a period of time which is much smaller, than that between acts of tunneling. As a result of the charging, the intrinsic mechanical stress leads to the Coulomb explosion. This problem was described in Ref. [20] for the solitary spherical cluster in absence of an external electric field. Extending these results, one can write the following expression

$$m\{(-\mu^g_{\mathrm{el(ion)}} + |e\eta V|)R/e + e/2\} \qquad (14)$$

for the critical electronic or ionic charge in quasi-classical approximation. Here $\mu^g_{\mathrm{el(ion)}}$ is the size-dependent electron (ion) chemical potential. For the range $V = (0, 2\ \mathrm{V})$ we have:

1) $\eta = 1$. Transitions of electrons between the emitter and the cluster occur more often, than between the cluster and the collector, therefore the electrons are ac-

cumulated on the cluster. In this case their maximal number is

$$n_{\max};\ -\mu_{\rm el}^{\rm g}R/e^2 + 1/2,$$

where $\mu_{\rm el}^{\rm g} = \mu_0 + \mu_1/R \equiv \mu^{\rm g}$ and $n_{\max}$; {+2.5,+6.5} for whole range of sizes {R}.

2) $\eta \approx 1$. Transitions of electrons between the cluster and the collector occur more often, than between the cluster and the emitter, therefore on the cluster the deficiency of electrons is observed. Using the definition of ion chemical potential (see Refs. [20, 25]), this number determines as

$$n_{\min} = (\mu_{\rm ion}^{\rm g} - |e\eta V|)R/e^2 - 1/2$$

and $n_{\min} \approx \{-4, -11\}$.

Similarly, for V = (–2,0 V) we have:

1) $n_{\min};\ \mu_{\rm ion}^{\rm g}R/e^2 - 1/2;\ \{-3.8, -10.6\}$.

2) $n_{\max} = (-\mu_{\rm el}^{\rm g} + |e\eta V|)R/e^2 + 1/2;\ \{+3,+8\}$.

Below, the *whole* numbers $[n_{\max}]$ and $[n_{\min}]$ bound the summation in (26). The effect of spectrum quantization can change these numbers no more than in ±1 according to (1) (see Ref. [20]).

Effective collision frequency of excited electrons in a cluster is defined as [31]

$$\frac{1}{\tau_\varepsilon} = \frac{1}{\tau} + \frac{v_F}{R},\ v_F = \frac{h}{mr_0}\left(\frac{9\pi}{4}\right)^{1/3}, \qquad (15)$$

where τ is a relaxation time in the bulk of the metal, caused by electron-electron collisions ($\tau \times 10^{14}$ = 6.23 s for Au at T = 75 K [32]), and v_F is the electron velocity at the Fermi surface in the bulk. The estimation performed in Ref. [33] gives a preferred electron collision on walls of a dot, therefore τ_ε; R/v_F. It leads to $\tau_\varepsilon \Delta\varepsilon_p/h$; {0.52,0.17}, i. e. to a broadening of levels. We assume that the electron thermalization occurs much faster than acts of tunneling. "New" electrons fill up a number of own electrons, changing their distribution and, accordingly, the chemical potential. This state of the cluster will be a starting state for the next act of tunneling.

6 BASIC ENERGY AND KINETIC RELATIONS

We assume, that the *total* energy of all three electrodes $\tilde{E}$ does not change during the tunneling. In the case of transition of δN electrons from the emitter to the granule (containing n "surplus" electrons), using Eq. (12) we have

$$\delta\tilde{E} = -\delta N\vec{\varepsilon}^{e} + \delta N\varepsilon_p + \frac{(-e)^2}{2C}[(n+\delta N)^2 - n^2] - e\delta N\eta^+ V = 0. \qquad (16)$$

In this expression we take into account that the δN electrons are ionized from the level $\vec{\varepsilon}^{\rm e}$ on the emitter (whose capacitance is equal to infinity) and then fill up the level ε_p in a granule with finite capacitance C.

By analogy with Ref. [34], using Eq. (12) and Eq. (16) for δN = 1, and then taking into account a contact potential difference (4), for emitter-granule transition we have

$$\vec{\varepsilon}^{\rm e} = \varepsilon_p' + \tilde{E}_C(n + 1/2) - e\eta^+ V, \qquad (17)$$

where $\varepsilon_p' \equiv \varepsilon_p - e\delta\phi$. The arrow on the top indicates the energies which are determined by transfers according to Fig. 1. We suppose, that $n \equiv n(V)$ and n = 0 at V = 0. However, the granule is charged by the charge $Q_{\rm eff}^0$ before voltage applied. Therefore, we assume that n is the result of the applied voltage only.

For granule-emitter transition we have

$$\vec{\varepsilon}^{\rm e} = \varepsilon_p' + \tilde{E}_C(n - 1/2) - e\eta^+ V. \qquad (18)$$

Similarly, for the granule-collector and collectorgranule transitions we have

$$\vec{\varepsilon}^{\rm c} = \varepsilon_p' + \tilde{E}_C(n \mp 1/2) + e(1-\eta^+)V. \qquad (19)$$

Here the upper/under arrows at the left correspond to the following signs on the right. Independently of n the relation

$$\vec{\varepsilon}^{\rm e} - \vec{\varepsilon}^{\rm e} = \tilde{E}_C = \vec{\varepsilon}^{\rm c} - \vec{\varepsilon}^{\rm c}$$

takes place. It agrees with well-known quasi-classical relation for the ionization potential and electron affinity,

$$IP - EA = E_C$$

(see, e. g. Ref. [20]). Thus, Eqs. (17)–(19) represent a golden rule approximation.

The tunneling of a single electron through barriers is determined by the tunnel rates $\Gamma^{\rm e,c}$, which depend on the junction geometry and the voltage fraction η. In general, their evaluation is far from a trivial problem [2, 27]. We assume that $\Gamma^{\rm e,c}$ are small and the temperature is not too low, i. e. $k_BT > h(\Gamma^{\rm e} + \Gamma^{\rm c}) = \min\{\Delta\varepsilon_p, \tilde{E}_C\}$.

By analogy with the theory of Ref. [29], we introduce the partial tunneling streams from electrodes to a granule

$$\overrightarrow{\omega_n^{\mathrm{e}}} = 2\sum_p \Gamma(\overrightarrow{\varepsilon^{\mathrm{e}}}) f(\overrightarrow{\varepsilon^{\mathrm{e}}} - \mu_V^{\mathrm{e}})[1 - f(\overrightarrow{\varepsilon^{\mathrm{e}}} - \overrightarrow{\mu_C^{\mathrm{e}}})], \quad (20)$$

$$\overleftarrow{\omega_n^{\mathrm{c}}} = 2\sum_p \Gamma(\overleftarrow{\varepsilon^{\mathrm{c}}}) f(\overleftarrow{\varepsilon^{\mathrm{c}}} - \mu_V^{\mathrm{c}})[1 - f(\overleftarrow{\varepsilon^{\mathrm{c}}} - \overleftarrow{\mu_C^{\mathrm{c}}})], \quad (21)$$

and from a granule to the electrodes

$$\overleftarrow{\omega_n^{\mathrm{e}}} = 2\sum_p \Gamma(\overleftarrow{\varepsilon^{\mathrm{e}}})[1 - f(\overleftarrow{\varepsilon^{\mathrm{e}}} - \overleftarrow{\mu_V^{\mathrm{e}}})] f(\overleftarrow{\varepsilon^{\mathrm{e}}} - \mu_C^{\mathrm{e}}), \quad (22)$$

$$\overrightarrow{\omega_n^{\mathrm{c}}} = 2\sum_p \Gamma(\overrightarrow{\varepsilon^{\mathrm{c}}})[1 - f(\overrightarrow{\varepsilon^{\mathrm{c}}} - \overrightarrow{\mu_V^{\mathrm{c}}})] f(\overrightarrow{\varepsilon^{\mathrm{c}}} - \mu_C^{\mathrm{c}}), \quad (23)$$

where the factor 2 takes into account the spin degeneration of levels in electrodes. In view of the applied voltage (and charging of a granule) the spectrums (see Eqs. (17)–(19)) and the chemical potentials are shifted in distributions (2) and (3),

$$-\mu_V^{\mathrm{e}} \equiv W_0^{\mathrm{e}}, \quad \overleftrightarrow{\mu_C^{\mathrm{e}}} = \mu^{\mathrm{g}} - e\delta\phi + \tilde{E}_C(n \mp 1/2) - e\eta^{+}V,$$
$$\overleftrightarrow{\mu_C^{\mathrm{c}}} = \mu - e\delta\phi + \tilde{E}_C(n \pm 1/2) - e(1-\eta^{+})V,$$
$$\mu_V^{\mathrm{c}} = \mu_0^{\mathrm{c}} - eV.$$

As the first approximation of the perturbation theory [20], for small V, μ^{g} is determined not only by the formal shift of the well depth, but also by the number of conduction electrons in the granule ($N = N_0 + n_{\mathrm{q}}$, $n_{\mathrm{q}} = n + [Q_{\mathrm{eff}}^0]/e$). The use of the chemical potentials is correct in a quasi-equilibrium state, i. e. when the intervals between acts of tunneling are much longer than the relaxation time. It is also supposed, that the external electric field and the Coulomb blockade do not remove degeneration of levels.

Let's denote the total electron streams from/to leads into/out the cluster, as

$$\omega_n^{\mathrm{in}} = \overrightarrow{\omega_n^{\mathrm{c}}} + \overleftarrow{\omega_n^{\mathrm{c}}}, \quad \omega_n^{\mathrm{out}} = \overleftarrow{\omega_n^{\mathrm{e}}} + \overrightarrow{\omega_n^{\mathrm{c}}}.$$

In the limit of weak tunneling, the probability P_n of the finding of n above mentioned electrons at central electrode is defined by the master equation in the stationary limit

$$\dot{P}_n = \omega_{n+1}^{\mathrm{out}} P_{n+1} + \omega_{n-1}^{\mathrm{in}} P_{n-1} - (\omega_n^{\mathrm{in}} + \omega_n^{\mathrm{out}}) P_n = 0. \quad (24)$$

The requirement of the stationarity gives the recurrent relation

$$P_{n+1} = P_n \frac{\omega_n^{\mathrm{in}}}{\omega_{n+1}^{\mathrm{out}}}. \quad (25)$$

The dc current flowing through a metallic quantum dot (with restriction on its instability (14)), is determined as

$$I = -e\sum_{n_{\min}<0}^{n_{\max}>0} P_n(\overrightarrow{\omega_n^{\mathrm{e}}} - \overleftarrow{\omega_n^{\mathrm{e}}}) = -e\sum_{n_{\min}<0}^{n_{\max}>0} P_n(\overrightarrow{\omega_n^{\mathrm{c}}} - \overleftarrow{\omega_n^{\mathrm{c}}}). \quad (26)$$

Let's consider the case of "strong quantization" for electron spectrum:

$$\Delta\varepsilon_p \gg E_C.$$

This regime is hypothetically reached by a significant increase of the cluster capacitance (the cluster shape must be changed to the needle-like or disk-like one under the condition that its volume is fixed (see, e.g. Ref. [20]). Thus the charge Q_{eff}^0 in (5), which provides a contact potential difference, is proportional to the capacitance and can have large magnitude. When the voltage is applied, the charge, which is caused by the transferring surplus electrons, is much less than Q_{eff}^0. Therefore it insignificantly have influence on the cluster energetics. In reality, the inequality $\Delta\varepsilon_p \gg \tilde{E}_C$ is not possible even for the long atomic chain [20]. Nevertheless, this case is useful from the methodical point of view to analyze the current gap of $I-V$ characteristics.

As an assumption, we use the fixed tunnel rates at the Fermi level in the emitter. It is correct for the small voltages, $eV = W_0$. Neglecting in (17)–(19) terms $\sim \tilde{E}_C$, it is easy to obtain the result, similar to Ref. [29]:

$$I = I_0 \sum_p [f(\varepsilon^{\mathrm{e}} - \mu_0^{\mathrm{e}}) - f(\varepsilon^{\mathrm{c}} - \mu_V^{\mathrm{c}})], \quad (27)$$

where $I_0 = 2e\Gamma^{\mathrm{e}}\Gamma^{\mathrm{c}}/(\Gamma^{\mathrm{e}} + \Gamma^{\mathrm{c}})$.

The expressions in this section are written down for $V > 0$. In the case $V < 0$, the $I(V)$ can be easily received, if we set $V = 0$ on a collector and $V > 0$ on the emitter, and use $\eta^{-} = 1 - \eta^{+}$.

In the general case, for calculation of $I-V$ (26) it is necessary to know probabilities P_n. Their statistical determination is a complicated problem [35, 36]. In the experiments, the size of the cluster and its location are known only approximately, therefore detailed calculations of P_n are not suitable. Using the recurrent relations we can find the ratios $P_{n\neq 0}/P_0$.

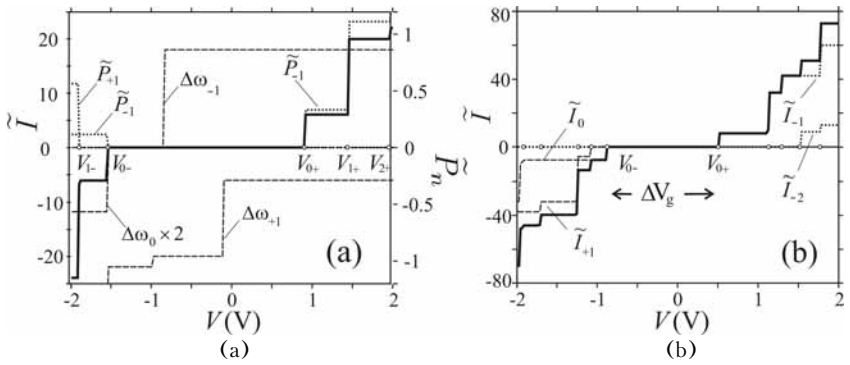

Figure 5 – The current-voltage curves (solid lines) and its components, calculated from Eq. (26) (β = 1, η^{+} = 0.1, T = 30 K). $\Delta\omega_n(V)$ is given in Γ^{e} units:
(a) $Au/Au_{40}/Au$; (b) $Au/Au_{100}/Au$

7 APPLICATION AND DISCUSSION

7.1 Thermal equilibrium

Setting the collector-granule distance d_c, parameter $\beta = \Gamma^{e}/\Gamma^{c}$ and using the recurrent relation (25) for Eq. (26), it is possible to calculate the reduced dc current $\tilde{I} \equiv I/(eP_0\Gamma^{e})$. We do not evaluate separately the threshold voltages, in our scheme it appears automatically.

The results of calculations of the $I-V$ characteristics for the structures $Au/Au_{N_0}/Au$, based on spherical clusters, are presented in Fig. 5. For completeness of analysis, the voltage behavior of the reduced probabilities $P_n(V) \equiv P_n/P_0$ and the difference of electron streams $\Delta\omega_n = \overrightarrow{\omega_n^{e}} - \overleftarrow{\omega_n^{e}}$ are given also.

The current jumps are stipulated by the jumps of $\tilde{P}_n(V)$ and $\Delta\omega_n(V)$, because the current is formed by their product. As one can surmise, the jump of probability $\tilde{P}_{-1}(V)$ causes the current jump in the threshold voltage V_{0+}.

Making use of the equality $\tilde{I} \equiv \sum_n \tilde{I}_n(V)$ in accordance with Eq. (26) one can fix also the "threshold" values of n. As is seen from Fig. 5 (b), the role of partial current components I_n (with $|n| > 1$) grow with increasing N_0. The charging leads to energy shift of spectrum according to Eqs. (17)–(19). Thus the different parts of a spectrum are involved during tunneling.

The current gap width ΔV_g for all structures is determined by values $n = 0, -1$. The probability P_{-1} prevails over P_{+1}, because the "granule-collector" electron stream is more than a "emitter-granule" one and the granule is charged positively (i. e. $n < 0$). For low temperatures ($k_B T^{g}_{eff} = \Delta\varepsilon_F$), the current gap width $\Delta V_g = V_{0+} + |V_{0-}|$ is determined analytically by the conductance gap boundaries V_{0-} and V_{0+}. For example, V_{0+} is defined from the condition of absence of collector current of the direct $\tilde{I}-V$ curve branch ($V > 0$), and finally we have:

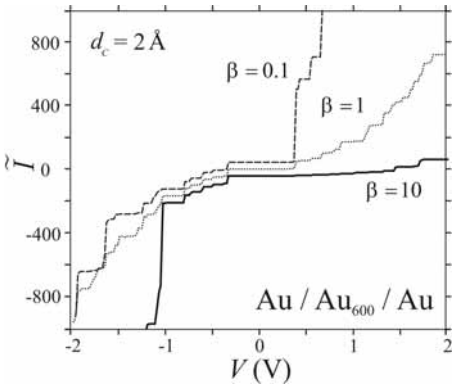

Figure 6 – Calculated $I-V$ curves at T = 30 K for structure based on spherical clusters. For presentation the curves are shifted slightly on a vertical

$$\Delta V_g = \left(\frac{1}{2e}\tilde{E}_C + \frac{1}{e}\Delta\varepsilon\right)\left[\frac{1}{2-\eta^{+}} + \frac{1}{2-\eta^{-}}\right], \qquad (28)$$

where $\Delta\varepsilon \equiv \mu^{g} - \varepsilon^{HO} \geq 0$ at T = 0. Calculated values of ΔV_g are in a good agreement with the experimental values based both on spherical and disc-shape clusters. For large granules $\Delta V_g \to 0$ as $R \to \infty$.

Within the applied voltage the $\tilde{I}-V$ characteristics versus η^{+} are shifted to the right and the gap width decreases a little. The calculated $I-V$ curves of the structure $Au/Au_{600}/Au$ for fixed η^{+} (d_c = 2 Å) and different β are shown in Fig. 6. The current gap is practically independent on β, however, the current jumps are strongly dependent on the value of β, which, in its turn, has no influence on threshold voltages.

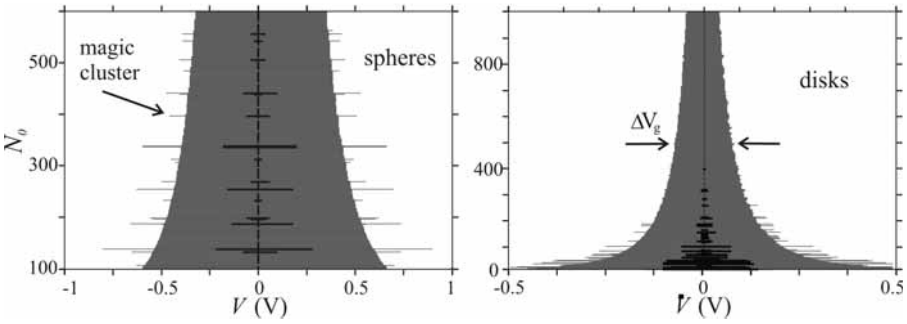

Figure 7 – The current gaps vs N_0 calculated from Eq. (26) (d_c = 2 Å and β = 10). Solid lines show the gaps calculated from Eq. (27) for the case of "strong quantization". For presentation the gaps are placed on a vertical

In order to illustrate our results, in Fig. 7, we compare the size dependences $\Delta V_g(N_0)$ calculated from Eqs. (26) and (27) for spheres and disks. The largest quantities ΔV_g correspond to the magic granules, for which $\Delta\varepsilon \neq 0$. For the case of "strong quantization" the size of current gap for non-magic clusters is equal to zero explicitly, because the emitter Fermi level is in line to the closed levels in cluster. Calculations demonstrate the non-monotonic dependence $\Delta V_g(N_0)$. These results shows also, that a charging leads to the growth of a gap.

The actual forms of dependence $\Delta V_g(d_c)$ for the structure based on magic disk Au_{178} ($R \approx 35$ Å) are plotted in Fig. 8. In experiments [14, 15] the gap varied as $0.8 \to 0.4 \to 0.7$ V for the cyclic variation of $d_c \approx 1 \to 2 \to 1$ Å. The reasons of such numerical distinction of our results, apparently consists in neglecting the role of nonlinearities in the strong electric field and in energy dependence of tunneling rates. At high rates the capacitance ceases to be classical and can strongly grow ($E_C \to 0$) [37, 38], showing non-monotonic dependence from Γ^c. It means, that in a reality we deal with the intermediate cases (between limiting estimations from Eqs. (26) and (27) in Fig. 8).

Let's discuss other features of the tunnel structure. In spite of the fact that the emitter and a collector are made of one material, the chemical potentials of electrons are not equal to each other: the emitter is represented by a thick film of Au (111), and a collector is a polycrystal of Au. Their work functions are different [39]. Except for it the emitter is covered with a dielectric film, that also influences a electron work function. We can estimate this contribution.

Proceeding from indirect measurements [40], the work function decreases with growth dielectric constant ϵ of coating. The calculations of the electron work function W_d for cylindrical nanowires in a dielectric confinement are done in Ref. [41]: W_d decreases approximately on 20 % at magnitude as ϵ rise from 1

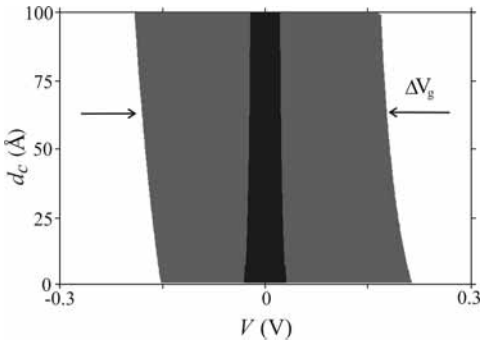

Figure 8 – The current gap vs d_c calculated from Eqs. (26) and (27) for magic disk Au_{178}, β = 10

to 4. The basic contribution thus can be related to the change of electrostatic dipole barrier which contribution to a work function of system gold-vacuum makes up to 30 % [39]. Hence, this contribution also makes a upper limit of the change of W_d for metal-dielectric-vacuum system. Owing to $W_d < W_0$ the inequality $|\mu^g| > W_d$ is possible, that can lead to negative charging of the cluster before the application of voltage.

7.2 A role of hot electrons

The consequence of the phonon spectrum deformation of granules is the weakening of the electron-phonon interaction within them: $v_F/R \gg \omega_D$, where v_F is the electron velocity at the Fermi surface in the bulk, and ω_D is the Debye frequency. This interaction can be so suppressed that the electron-electron interaction becomes the main mechanism for the dissipation of the energy, which is injected to the particle. This additional energy results in the overheating of the electron subsystem, which is described by the Fermi statistics with some effective (enhanced) temperature T^g_{eff}, and the temperature of the ion subsystem only slightly changes [42, 7, 8, 9]. With the increase of the bias voltage V, the number of electrons, relaxing in the granule, increases significantly.

Among them are all the electrons with energies in the interval $e\eta V$ below the Fermi level of the granule (ηV is the fraction of the bias voltage on the granule), since the "flow" of tunneling electrons increases from below lying levels, thereby, involving large num-ber of conductivity electrons to the relaxation process. At the same time, channels of losses appear, which are related to the generation of holes on the occupied levels and their subsequent recombination. The granule does not fragmentize at the significant overheating of the electron subsystem, because the $I-V$ curves are reproduced at the cyclic changes of the bias voltage [14, 13].

The estimate of the energy, which is pumped by the conductivity electrons to the granules of discontinuous films, is given in Ref. [7] ($\sim 0.2,0.3$ eV). This means that the experiments [14, 13] correspond to the Coulomb blockade regime in the region of current gap at the whole diapason of R and reasonable values of T^{g}_{eff}. Also, the quantum ladder can be smeared out by the thermal fluctuations,

$$E_C > \Delta\varepsilon_F > k_B T^{e,c,g},$$

where $\Delta\varepsilon_F$ is the difference between discrete levels in the vicinity of the granule Fermi level, and $\Delta\varepsilon_F = \Delta\varepsilon_p$ for magic clusters at $T = 0$ (see Fig. 2). We represent the emitter and the collector as the electron reservoirs with continuum spectrums and temperatures $T^{e,c}$ equal to the thermostat one. The spectrum of states is calculated in advance and, therefore, the chemical potential of neutral Au_{N_0} granules and its temperature dependence can be found from equation (3) at a given temperature T^{g}_{eff}.

For the comparison with the results of Refs. [14, 13], the calculations are done for three temperatures of the collector and emitter $T^{e} = T^{c} = 5, 30, 300$ K, and also $T^{g}_{eff} = T^{e}, 2000$ K. The values $\Gamma^{c} = \Gamma^{e} = 1$ and $\eta = 1/2$ are used for all cases.

Fig. 9 shows calculated $I-V$ curves for disc of radius R = 20 A (magic cluster Au_{230}) and sphere of radius R = 10 A (magic cluster Au_{256}). The calculation of the $\tilde{I}-V$ curves and current gap can be done only numerically at $k_B T^{g}_{eff} \geq \Delta\varepsilon_F$, when the larger part of the spectrum, compared to $\Delta\varepsilon_F$, is responsible for the charge transfer. Our calculations show an evident dependence of $\tilde{I}-V$ curves flatness on the electron subsystem temperature.

However, it order to obtain an agreement with observed $I-V$ curves it is necessary to suggest that electrons in the emitter and collector are also heated up to some effective temperature, which is higher than the thermostat one. It is possible, because electrons (the current I = 1 pA is provided by $I/e \sim 10^6$ number of electrons per second) relax in generally on the free path length in the last electrodes.

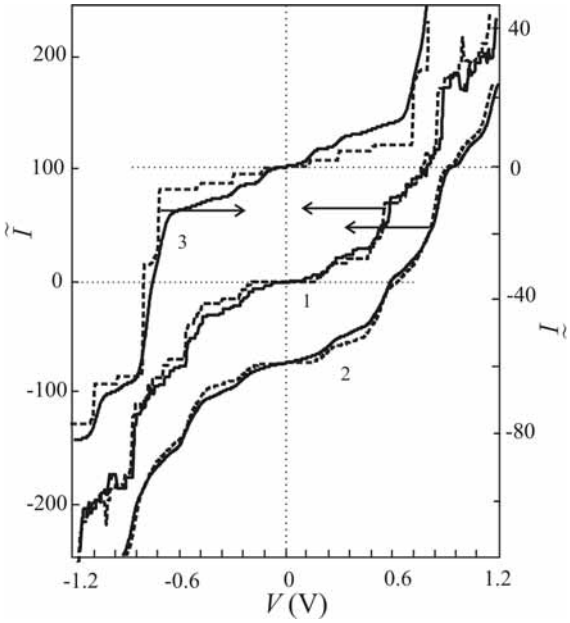

Figure 9 – Calculated $\tilde{I}-V$ curves of structure based on magic clusters: disc Au_{230} and sphere Au_{256}

1 – Au_{230}: dotted curve – $T^{e,c,g}$ = 5 K,
solid – $T^{e,c}$ = 5 and $T^{e,c,g}$ = 300 K
2 – Au_{230}: dotted curve – $T^{e,c,g}$ = 300 K,
solid – $T^{e,c}$ = 300 and T^{g}_{eff} = 2000 K
3 – Au_{256}: dotted curve – $T^{e,c}$ = 30 K and T^{g}_{eff} = 2000 K,
solid – $T^{e,c}_{eff}$ = 300 and T^{g}_{eff} = 2000 K

For the illustration, we present our result at Fig. 9 for the sphere at $T^{e,c}$ = 300 K and T^{g}_{eff} = 2000 K. Only by such a way, we can explain the flattening of the $I-V$ curves for the metallic cluster structures at low thermostat temperatures. With the increase of the bias voltage, the current flow is accompanied by the increase of the electron gas temperature.

8 SUMMARY

In the framework of the particle-in-a-box model for the spherical and disk-shaped gold clusters, the electron spectrum was computed. In this model, the work function of clusters is smaller that of semi-infinite gold electrodes. It resulted in the appearance of a contact potential difference between a cluster and electrodes. Residual effective charge is equal to non-integer elementary charge e, which is analogous to the charge of cluster in "chemisorption regime". For the small spherical clusters, positive charge is less than e. However, this charge can accept a values larger than e for the disks of monatomic thickness. Additional charging of the clusters can lead to the Coulomb instability, because it is close to a critical charge. The charging results in the energy shift of the spectrum.

The current-voltage characteristics were analyzed taking into account the contact potential difference. For single-electron molecular transistors based on the small gold clusters the current gap and its voltage asymmetry were computed. The largest gaps correspond to the magic granules. For the case of "strong quantization", the size of a current gap for non-magic clusters is equal to zero explicitly, because the emitter Fermi level is in line to the closed levels in cluster. We derive the simple expression for the size dependence of the current gap width, which taking into account the Coulomb blockade and discreteness of the energy levels. The results shows, that a charging leads to the growth of a gap.

In conclusion, we have calculated the $I-V$ characteristics of structure based on magic clusters: disc Au_{230} and sphere Au_{256}. We have suggested that the overheating of electron subsystem leads to the disappearance of current gap and significant flattening of current-voltage curves. Our results are in a good qualitative agreement with experiment of Ref. [14, 13].

APPENDIX A. ELECTRON SPECTRUM IN CYLINDRICAL-LIKE CLUSTERS

As an approximation, the profile of the one-electron effective potential in the cluster can be represented as a potential well of the depth $U_0 < 0$. The three-dimensional Schrödinger equation for a quantum box can be separated to the one-dimensional equations. The spectrum of wave numbers in a spherical and cylindrical potential wells are determined from the continuity condition of a logarithmic derivative of the wave function on the boundaries. For a disk of radius R and thickness H it is necessary to solve numerically the equation:

$$k_{nm}\frac{I'_m(k_{nm}R)}{I_m(k_{nm}R)} = \kappa_{nm}\frac{K'_m(\kappa_{nm}R)}{K_m(\kappa_{nm}R)}. \qquad (A.1)$$

Here I_m is the Bessel function, K_m is the McDonald function, the stroke denotes a derivative over an argument, $k_{nm} = \sqrt{k_0^2 - \kappa_{nm}^2}$, $k_{nm} = \sqrt{k_0^2 - \kappa_{nm}^2}$, $\hbar k_0 = \sqrt{2m_e|U_0|}$, and m_e is the electron mass. The $n = 1, 2, 3, \ldots$ number the roots of the Eq. (29) for the fixed $m = 0, \pm1, \pm2, \ldots$.

Quantization of the wave vector k_s along the cylinder axis is determined by the solution of the equation:

$$k_s H = s\pi - 2\arcsin(k_s/k_0),$$

where s is the integer number. Neglecting the area near cylinder edges, the energy spectrum is calculated by a simple way as follows

$$\varepsilon_{nms} = U_0 + \frac{h^2}{2m_e}(k_{nm}^2 + k_s^2).$$

In addition to the spin degeneration, there is a double degeneration with respect to the sign of index m, since $k_{n,m} = k_{n,-m}$. Further, the spectrum of cluster is denoted as ε_p, $p = 1, 2, 3\ldots$ is the number of *one-electron state*. All levels are numbered in order to increase energies.

APPENDIX B. ENERGY OF CLUSTER IN EXTERNAL ELECTRICAL FIELD

Using spherical coordinates, we remove the center point $z = 0$ from emitter in a center of a granule, and we direct a z axis from a collector to the emitter under the conservation of the potential difference between them. Then an electric field $E = |E|z$, where z is a unit vector along an z axis.

As the surplus charge is effectively distributed over a surface, it is quite reasonable for estimation to use the form

$$\delta n_1(r) = \begin{cases} 0, & 0 < r < R - b, \\ \tilde{n}, & R - b < r < R, \\ 0, & R > 0. \end{cases} \qquad (B.1)$$

Using condition (8), we obtain the following expression for surface concentration

$$\tilde{n} = \frac{\Delta N}{\Omega(3\xi - 3\xi^2 + \xi^3)},$$

where $\Omega = 4\pi R^3/3$, and $\xi = b/R$ is the small parameter.

Then, we use the linear response approach (see, e. g. Ref. [30])

$$\delta n_2(r, \theta) = Y(r)|E|\cos\theta. \qquad (B.2)$$

The spherically symmetric function $Y(r)$ in (31) are determined from the normalization condition (9) and a global minimum of the functional, $\delta\tilde{E}[n(r)] \to 0$.

One of the terms, interesting for us, is

$$-e\int \delta n_1(r)\varphi(z)d^3r,$$

where φ is an external electrostatic potential. In the case of $V > 0$ and vacuum collector-emitter space $\varphi(z) = V(z - d_e - L/2)/d$, where $d = d_e + L + d_c$. After the integration in spherical coordinates, the term, which is proportional to z, vanishes, and, as a result, we have $-e\Delta N\eta V$, η is a fraction of a voltage.

Other three terms

$$\int \frac{\delta n_1(\mathbf{r})\delta n_2(\mathbf{r}') + \delta n_1(\mathbf{r})\delta n_1(\mathbf{r}') + \delta n_2(\mathbf{r})\delta n_2(\mathbf{r}')}{|\mathbf{r}-\mathbf{r}'|} d^3r d^3r'. \quad \text{(B.3)}$$

give a basic contribution to the second order of expansion (10). The first integral in Eq. (32) for the functions (30) and (31) vanishes after the integration on corners and second one equals

$$(\Delta N)^2 \frac{E_C}{2}\left(1 + \frac{1}{3}\xi + O(\xi^2)\right).$$

The third integral was calculated earlier for definition of the polarizability of a cluster $\alpha = -(4\pi/3)\int_0^\infty Y(r) r^3 dr \equiv R_{\text{eff}}^3 \approx R^3$ [30]. Finally, using $\xi \to 0$, we obtain Eq. (12).

REFERENCES

1. *Likharev, K. K.* SET: Coulomb blockade devices [Text] / K. K. Likharev // Nano et Micro Technologies. – 2003. – V. 3. – P. 71–114.
2. *Von Delft, J.* Spectroscopy of discrete energy levels in ultrasmall metallic grains [Text] / J. von Delft, D. C. Ralph // Phys. Rep. – 2001. – V. 345. – № 1. – P. 61.
3. *Aleiner, I. L.* Quantum Effects in Coulomb Blockade [Text] / I. L. Aleiner, P. W. Brouwer, L. I. Glazman // Phys. Rep. – 2002. – V. 358. – P. 309.
4. *Otero, R.* Observation of preferred heights in Pb nanoislands: A quantum size effect [Text] / R. Otero, A. L. Vazquez de Parga, R. Miranda // Phys. Rev. B.– 2002. – V. 66. – id. 115401.
5. *Semrau, S.* Designable electron transport features in one-dimensional arrays of metallic nanoparticles: Monte Carlo study of the relation between shape and transport [Text] / S. Semrau, H. Schoeller, W. Wenzel // Phys. Rev. B. – 2005. – V. 72. – id. 205443.
6. *Pogosov, V. V.* Introduction to Physics of Charged and Size Effects: Surface, Clusters, and Low-Dimensional Systems [Text] / V. V. Pogosov. – Moscow: Fizmatlit, 2006. – 328 p.
7. *Fedorovich, R. D.* Electron and light emission from island metal films and generation of hot electrons in nanoparticles [Text] / R. D. Fedorovich, A. G. Naumovets, P. M. Tomchuk // Physics Reports, 2000. – V. 328. – P.73-79.
8. *D'Agosta, R.* Local Electron Heating in Nanoscale Conductors [Text] / R. D'Agosta , Na Sai, Di Ventra Massimiliano // Nanoletters. – 2006. – V. 6. – № 12. – P. 2935–2938.
9. *Galperin, M.* Heat conduction in molecular transport junctions [Text] / M. Galperin, M. Ratner, A. Nitzan // Phys. Rev. B. – 2007. – V. 75. – id. 155312.
10. *Millo, O.* Charging and quantum size effects in tunnelling and optical spectroscopy of CdSe nanorods [Text] / O. Millo, D. Katz, D. Steiner et al. // Nanotechnology. – 2004. – V. 15. – P. 1–6.
11. *Ohgi, T.* Charging effects in gold nanoclusters grown on octanedi-thiol layers [Text] / T. Ohgi, H. Y. Sheng, Z. C. Dong, H. Nejoh, D. Fujita // Appl. Phys. Lett. – 2001. – V. 79. – P. 2453.
12. *Ohgi, T.* Consistent size dependency of core-level binding energy sifts and single electron tunneling effects in supported Au nanoclusters [Text] / T. Ohgi, D. Fujita // Phys. Rev. B. – 2002. – V. 66. – id. 115410.
13. *Ohgi, T.* Capacitance dependence of chemical potential distribution in supported nanoclusters [Text] / T. Ohgi, Y. Sakotsubo, D. Fujita, Y. Ootuka // Surface Science. – 2004. – V. 402. – P. 566–568.
14. *Wang, B.* Single-electron tunneling study of two-dimensional gold clusters [Text] / B. Wang, X. Xiao, X. Huang // Appl. Phys. Lett. – 2000. – V. 77. – № 8. – P. 1179.
15. *Hou, J. G.* Nonclassical behavior in the capacitance of a nanojunction [Text] / J. G. Hou, B. Wang, J. Yang // Phys. Rev. Lett. – 2001. – V. 86. – № 13. – P. 5321.
16. *Boyen, H.-G.* Alloy formation of supported gold nanoparticles at their transition from clusters to solids: Does size matter? [Text] / H.-G. Boyen, A. Ethirajan, G. Kastle et al. // Phys. Rev. Lett. – 2005. – V. 94. – id. 016804.
17. *Hou, J. G.* Detecting and manipulating single molecules with STM [Text] / J. G. Hou, A. Zhao // NANO: Brief Rep. Rev. – 2006. – V. 1. – P. 15.
18. *Pogosov, V.* Effects of charging and tunnelling in a structure based on magic and non-magic metal clusters [Text] / V. Pogosov, E. Vasyutin // Nanotechnology.– 2006. – V. 17. – P. 3366–3374.
19. *Soldatov, E. S.* Room temperature molecular single-electron transistor [Text] / E. S. Soldatov, V. V. Khanin, A. S. Trifonov, S. P. Gubin, V. V. Kolesov, D.E. Presnov, S. A. Iakovenko, G. V. Khomutov, A. N. Korotkov // Physics-Uspekhi. – 1998. – V. 41. – P. 202.
20. *Pogosov, V.* Energetics of metal slabs and clusters: the rectangle-box model [Text] / V. Pogosov, V. Kurbatsky, E. Vasyutin // Phys. Rev. B. – 2005. – V. 71. – id.195410.
21. *Brack, M.* Metal clusters and magic numbers [Text] / M. Brack // Sci. Amer. – 1997. – V. 277. – P. 30.
22. *Gubin, S. P.* Molecular clusters as building blocks for nanoelectronics: the rst demonstration of a cluster single-electron tunnelling transistor at room temperature [Text] / S. Gubin, Y. Gulayev, G. Khomutov et al. // Nanotechnology. – 2002. – V. 13. – № 1. – P. 185–194.
23. *Kurkina, L. I.* Electron structure and chemical potential of small jellium clusters at nonzero temperatures [Text] / L. I. Kurkina, O. V. Farberovich // Sol. St. Commun.– 1996. – V. 98. – P. 469.
24. *Pogosov, V. V.* Sum-rules and energy characteristics of small metal particle [Text] / V. V. Pogosov // Sol. St. Commun. – 1990. – V. 75. – P. 469.
25. *Kiejna, A.* On the temperature dependence of the ionization potential of self-compressed solid- and liquid-metallic clusters [Text] / A. Kiejna, V. V. Pogosov // J. Phys.: Condens. Matter. – 1996. – V. 8, № 23. – P. 4245.
26. *Pogosov, V. V.* On some tenzoemission effects of the small metal particles [Text] / V. V. Pogosov // Sol. St. Commun. – 1992. – V. 81. – P. 129.
27. *Azbel', M. Ya.* Time, tunneling and turbulence [Text] / M. Ya. Azbel' // Phys. Uspekhi. – 1998. – V. 41. – P. 543.
28. *Parthasarathy, R.* Percolating through networks of random thresholds: Finite temperature electron tunneling in metal nanocrystal arrays [Text] / R. Parthasarathy, X.-M. Lin, K. Elteto et al. // Phys. Rev. Lett. – 2004. – V. 92, № 7. – id.076801.
29. *Averin, D.* Theoryof single–electron charging of quantum wells and dots [Text] / D. V. Averin, A. N. Korotkov, K. K. Likharev // Phys. Rev. B. – 1991. – V. 44.– № 12. – P. 6199.
30. *Snider, D. R.* Density-functional calculation of the static electronic polarizability of a small metal sphere [Text] / D. R. Snider, R. S. Sorbello // Phys. Rev. B. – 1983. – V. 28. – № 10. – P. 5702.
31. *Wood, D. M.* Quantum size effects in the optical properties of small metallic particles [Text] / D. M. Wood, N. W. Ashcroft // Phys. Rev. B. – 1982. – V. 25. – № 10. – P. 6255–6273.
32. *Sokolov, A. V.* Optical Properties of Metals [Text] / A. V. Sokolov. – New York : American Elsevier, 1967. – 311 p.
33. *Kurbatsky, V. P.* Optical low-frequency absorption of small metal particles [Text] / V. P. Kurbatsky, V. V. Pogosov // Techn. Phys. Lett. – 2000. – V. 26. – P. 1020.
34. *Beenakker, C. W. J.* Theory of Coulomb-blockade oscillations in the conductance of a quantum dot [Text] / C.W. J. Beenakker // Phys. Rev. B. – 1991. – V. 44. – № 4. – P. 1646.

35. *Brack, M.* Thermal properties of the valence electrons in alkali metal clusters [Text] / M. Brack, O. Genzken, K. Hansen // Z. Phys. D. – 1991. – V. 21. – P. 65.
36. *Petrov, E. G.* Kinetic rectification of charge transmission through a single molecule [Text] / E. G. Petrov, V. May, P. Hänggi // Phys. Rev. B. – 2006. – V. 73. – id.045408.
37. *Wang, J.* Capacitance of atomic junctions [Text] / J. Wang, H. Guo, J.–L. Mozos et al. // Phys. Rev. Lett.– 1998. – V. 80. – P. 4277.
38. *König, J.* Strong tunneling in the single-electron box [Text] / J. König, H. Schoeller // Phys. Rev. Lett. – 1998. – V. 81. – P. 3511.
39. *Pogosov, V. V.* Effect of deformation on surface characteristics of finite metallic crystals [Text] / V. V. Pogosov, O. M. Shtepa // Ukr. Phys. J. – 2002. – V. 47. – № 11. – P. 1065.
40. *Modinos, A.* Field, Thermionic and Secondary Electron Emission Spectroscopy [Text] / A. Modinos.– New York : Plenum Press, 1984. – 375 p.
41. *Smogunov, A. N.* Electronic structure of simple metal whiskers [Text] / A. N. Smogunov, L. I. Kurkina, S. I. Kurganskii, O. V. Farberovich // Surf. Sci. – 1997. – V. 391. – P. 245.
42. *Shklovskii, V. A.* The role of electrons of conductivity in forming of thermal resistance at border metal - dielectric [Text] / V. A. Shklovskii // Let. J. Exper. Theor. Phys. – 1977. – V. 26. – P. 679.

Надійшла 02.02.2009

Теоретически исследованы эффекты зарядки и одноэлектронного туннелирования в структуре на кластере. В рамках модели бесконечной потенциальной ямы для сферических и дискообразных золотых кластеров вычислены электронный спектр и температурная зависимость химического потенциала. Разница между химическими потенциалами массивных электродов и островков приводит к зарядке последних. Мы показываем, что эффективный остаточный заряд не равен целому значению заряда электрона e и зависит от формы кластера. Уравнения для анализа вольт-амперной характеристики используются с учетом ограничений, связанных с кулоновской неустойчивостью кластера. Для одноэлектронных молекулярных транзисторов вычислены немонотонные размерные зависимости токовой щели и ее асимметрия по напряжению. Мы предполагаем, что перегрев электронной подсистемы приводит к исчезновению токовой щели и постепенному сглаживанию вольт-амперных характеристик, что наблюдается в экспериментах.

Теоретично досліджені ефекти зарядки й одноелектронного тунелювання в структурі на кластері. У рамках моделі нескінченної потенційної ями для сферичних і дискообразних золотих кластерів обчислені електронний спектр і температурна залежність хімічного потенціалу. Різниця між хімічними потенціалами масивних електродів і острівців приводить до зарядки останніх. Ми показуємо, що ефективний залишковий заряд не дорівнює цілому значенню заряду електрона e й залежить від форми кластера. Рівняння для аналізу вольт-амперної характеристики використовуються з урахуванням обмежень, пов'язаних з кулоновською нестійкістю кластера. Для одноелектронних молекулярних транзисторів обчислені немонотонні розмірні залежності струмової щілини і її асиметрія по напрузі. Ми припускаємо, що перегрів електронної підсистеми приводить до зникнення струмової щілини й поступового згладжування вольт-амперних характеристик, що спостерігається в експериментах.

УДК 537.874.6

Я. В. Чумаченко, В. П. Чумаченко

К ОБОСНОВАНИЮ ЧИСЛЕННОГО РЕШЕНИЯ ОДНОЙ ЗАДАЧИ РАССЕЯНИЯ ВОЛН ДЛЯ НАГРУЖЕННОГО ИЗЛОМА ПРЯМОУГОЛЬНОГО ВОЛНОВОДА

Рассматривается полученное ранее решение задачи рассеяния волн в H-плоскостном 90°-изломе прямоугольного волновода, нагруженном диэлектриком. Исследована бесконечная система линейных алгебраических уравнений задачи. Установлена возможность ее решения методом усечения.

ВВЕДЕНИЕ

В последние годы метод произведения областей (ПО) успешно использовался для анализа ряда устройств волноводной техники. Укажем в качестве примера работы [1–3], где исследовались структуры различные по геометрии и назначению. В работе [4] метод был применен для решения задачи рассеяния волн в нагруженном H-плоскостном 90°-изломе прямоугольного волновода. Бесконечная система линейных алгебраических уравнений (СЛАУ) задачи решалась численно путем ее замены конечным числом уравнений. В настоящей статье приводится формальное обоснование применимости использованного метода усечения. Такое обоснование представляется важным, так как сходные матричные операторы появляются при применении метода ПО к исследованию и других узлов, в которых граничные поверхности пересекаются под прямым углом (как, например, в T-соединениях и крестообразных соединениях прямоугольных волноводов).